land

MDPI

Article

Spatiotemporal Evolution of Soil Erosion and Its Driving Mechanism in the Mongolian Section of the Yellow River Basin

Tian Tian [1,2,3,†], Zhenqi Yang [1,2,†], Jianying Guo [1,2,*], Tiegang Zhang [1,2], Ziwei Wang [1,2,3] and Ping Miao [4]

[1] Yinshanbeilu National Field Research Station of Steppe Eco-Hydrological System, China Institute of Water Resources and Hydropower Research, Beijing 100038, China
[2] Institute of Water Resources for Pastoral Area, Ministry of Water Resources, Hohhot 010020, China
[3] Desert Science and Engineering College, Inner Mongolia Agricultural University, Hohhot 010018, China
[4] Ordos River and Lake Protection Center, Erdos 017200, China
* Correspondence: guojy@iwhr.com; Tel.: +86-158-4938-9759
† Tian Tian and Zhenqi Yang are co-frist authors.

Abstract: Soil erosion is a popular environmental issue that threatens sustainability. Influenced by multiple factors, such as climate, soil, and terrain, Baotou City, which is in the Bohai Sea Economic Circle and the Economic Belt along the Yellow River, has a severe ecological environment. In this study, revised soil and soil wind erosion equations were used to evaluate the soil erosion dynamics in Baotou City, and the potential driving factors of soil erosion were further investigated. Results showed that from 1990 to 2020, the water erosion modulus in Baotou City increased first, decreased, and then increased, with great fluctuations in annual changes. The wind erosion modulus decreased continuously, with a small fluctuation in annual changes. Water erosion in 2020 was more severe, with 4840.5 km^2 added to the desert steppe and 1300.5 km^2 reduced in the Yellow River Basin. The extent of wind erosion was significantly reduced, and the phenomenon of wind erosion improved. Meteorological factors are the primary factors that influence soil water erosion and soil wind erosion. Meanwhile, adverse climate changes can alter physical and chemical soil properties and vegetation coverage, thereby indirectly influencing soil erosion. With the implementation of the Beijing–Tianjin sandstorm source control, the farmland return to forest project, the ecological restoration and protection project at the southern and northern foothills of Daqingshan Mountains, grazing prohibition, and rotation grazing—including grassland awards, subsidies, and other policies and systems during this period—the overall deteriorating trend of the grassland ecological environment in Baotou was contained, grassland ecological system functions were improved, wind and sand erosion was prevented, biodiversity was maintained, and the ecological service functions of soil and water conservation were guaranteed.

Keywords: grassland regions in Northern China; soil wind erosion; soil water erosion; Baotou City; ecological engineering

Citation: Tian, T.; Yang, Z.; Guo, J.; Zhang, T.; Wang, Z.; Miao, P. Spatiotemporal Evolution of Soil Erosion and Its Driving Mechanism in the Mongolian Section of the Yellow River Basin. *Land* **2023**, *12*, 801. https://doi.org/10.3390/land12040801

Academic Editor: Vincent Chaplot

Received: 21 February 2023
Revised: 27 March 2023
Accepted: 29 March 2023
Published: 31 March 2023

1. Introduction

Soil erosion refers to the structural failure, separation, movement, and deposition of soil and its parent material under external force. Soil erosion is one of the global environmental issues that restrict the sustainable development of human society [1–4]. On the one hand, the nutrient loss caused by soil erosion may decrease the yield. On the other hand, it erodes sediments delivered to streams and rivers, resulting in the siltation and disruption of aquatic ecosystem services. Channel aggradation associated with sedimentation may make rivers prone to flooding. Moreover, the soil erosion process may restrict the response of the soil ecosystem to climate changes and thereby influence the safety of the ecological environment [5]. The sustainable development goals of the United Nations recognize the importance of soil resources for sustainable development and promote and protect soil resources to realize the great ambition of zero land degradation by 2030 [6–8]. In Northern

China, the uneven distribution of climate, such as the difference between wet and dry due to the locations of the land and sea, and unreasonable human activities (grazing and coal mining), have accelerated the deterioration of the ecological environment, resulting in serious problems, such as soil and water loss and land desertification [9,10].

In general, soil wind erosion is associated with (semi)arid regions, whereas soil water erosion usually occurs in wet regions. Nevertheless, soil wind erosion and soil water erosion have significant influences on soil erosion in some arid or semi-arid regions and sometimes occur at the same time. Hence, soil erosion assessment, which focuses on only one stress, may provide incomplete information and be invalid for soil erosion control. The wind–soil water erosion coupling effect strengthens the probability of soil water erosion. Moreover, the transportation, erosion, and deposition of surface materials caused by soil wind erosion can provide materials for soil water erosion to occur again, thereby directly influencing the transformation of erosion substances [11,12]. Owing to windy and sandstorm weather during spring and rainy weather during summer and autumn in Northern China, soil water erosion and soil wind erosion occur alternately; however, they overlap in space, thus prolonging the period of erosion and intensifying the degree of soil erosion [13]. The mechanisms responsible for soil erosion are complicated. Identifying the internal driving forces of soil erosion is critical for the formulation of water and soil conservation policies. The mountain topography makes it difficult or impossible to conduct field surveys; hence, the quantitative assessment of soil erosion is carried out using the soil erosion forecast model.

Baotou City is located upstream of the Yellow Sea and in the hinterland of the Bohai Sea Economic Circle and the Economic Belt along the Yellow River. It is at the south end of the Mongolian Plateau, north of Northern China, and at the center of Inner Mongolia; it is next to the Yellow River, which flows to the south. The Yin Mountains run through the center of Baotou City, forming a plateau in the north, a mountainous region in the middle, and a plain in the south. The Yellow River Basin is an important ecological region in China, and its ecological protection and high-quality development were officially incorporated into the national key development strategies in 2019. In the Yellow River Basin, the ecological environment is vulnerable, and water security is facing severe challenges [14]. Since the 1950s, many management projects in the Yellow River Basin, such as small basin management, afforestation, and farmland return to forest, have achieved significant effects. However, regional differences remain in terms of the degree of land management [15,16]. Influenced by the natural environment and man-made interferences, a series of problems that influence ecological environmental safety, such as grassland desertification and soil–water loss, have emerged in Baotou City. Meanwhile, the unique terrain of the city contributes to the successive occurrences of soil water erosion and soil wind erosion. On this basis, soil modulus inversion is carried out on soil water erosion and soil wind erosion using the Revised Universal Soil Loss Equation (RUSLE) and the Revised Wind Erosion Equation (RWEQ) model to explore the spatiotemporal distribution patterns of the soil wind erosion and soil water erosion dynamics and disclose the major features and influencing factors of soil erosion changes. The results provide a reference for the quantitative assessment of soil–water loss, wind prevention, and sand fixation in Baotou City and substantially facilitate ecosystem protection and sustainability.

2. Materials and Methods

2.1. Study Area

Baotou City is located in Northern China (109°51′–111°25′ E, 40°15′–42°45′ N), covering an area of 27,768 km^2. In Baotou City, the mountainous area, the hilly grassland, and the plain account for 14.49%, 75.51%, and 10% of the total area, respectively. Baotou City is adjacent to Hohhot City to the east, connects with Bayannur to the west, borders Mongolia to the north, and faces Erdos City to the south, separated by the Yellow River (Figure 1). Baotou City is an important hub that connects Northern China and Northwestern China—a key emerging development region in Inner Mongolia—the central city of

Huhehaote–Baotou–Yinchuan Economical Zone, and Huhehaote–Baotou–Hubei Economic Circle. The basin area of the Yellow River system is 8579.44 km^2. Except for the Yellow River that runs through it, the rest of the rivers are internal rivers. The city has 76 rivers, all of which flow to the Yellow River from north to south. Baotou City exhibits a semi-arid mesotemperate continental monsoon climate, and the annual precipitation amounts to 175–400 mm, with great annual changes. The precipitation is concentrated in summer, that is, from July to September. The northwest wind plays a dominant role throughout the year, and the average wind velocity is 3.4 m/s. Soil conditions are poor, manifested by serious soil salinization, soil wind erosion-induced desertification, and soil–water loss.

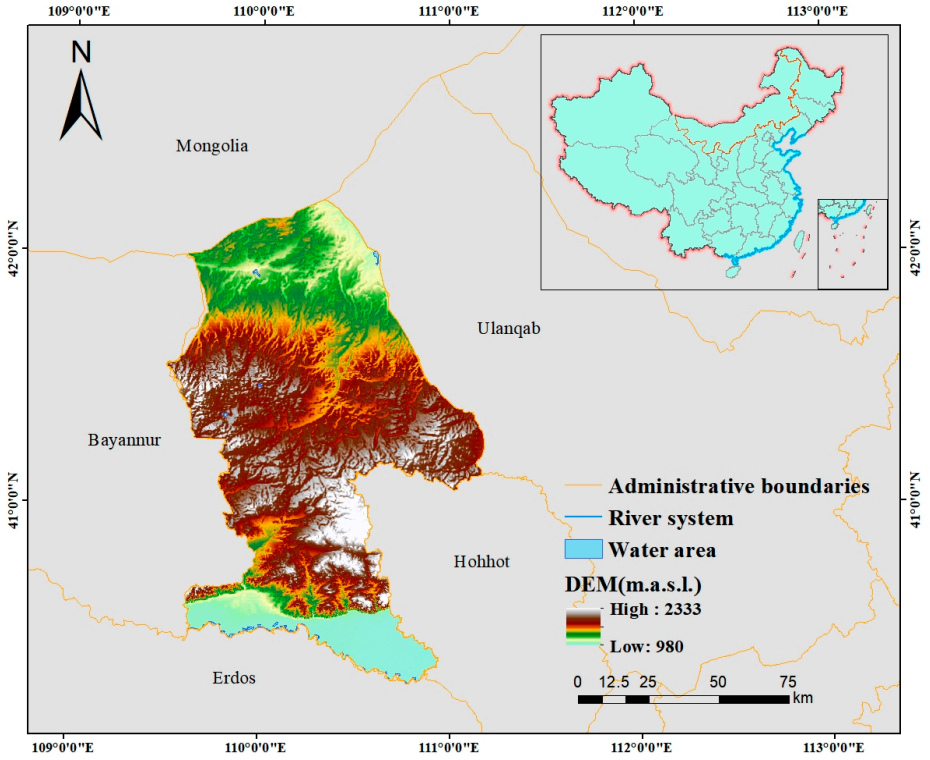

Figure 1. Study area.

2.2. Data Source and Processing

The basic data in this study included land-use-cover data from 1990, 1995, 2000, 2005, 2010, 2015, and 2020 and the vector diagram of the administrative boundaries of Baotou City; the Digital Elevation Model (DEM); the Normalized Difference Vegetation Index (NDVI); and meteorology, soil type, physical and chemical soil properties. Specifically, land-use data were obtained from the remote-sensing interpretation of Landsat4-5TM/Landsat8OLI images with a resolution of 30 m and cloud cover of less than 2%, which were downloaded from the geospatial data cloud (http://www.gscloud.cn/, accessed on 17 December 2022). NDVI data were obtained through waveband calculation using remote-sensing images. Data on multiple meteorological factors, including monthly precipitation, average air temperature, and average wind velocity, came from the National Science and Technology Infrastructure Platform—National Earth System Science Data Center (http://www.geodata.cn, accessed on 17 December 2022). Data on soil types and physical and chemical properties came from the global soil database Harmonized World Soil Database (HWSD) provided by the National Scientific Data of the Qinghai–Tibet Plateau (https://data.tpdc.ac.cn, accessed on 17 December 2022), which covers 11 terms of soil general information and 34 soil properties. The snow depth sources came from the National Scientific Data of the Qinghai–Tibet Plateau (https://data.tpdc.ac.cn, accessed on 17 December 2022), and the snow cover factor data were calculated based on acquired long-time series data.

2.3. Research Methods

2.3.1. Soil Water Erosion Model

In the 1980s, Chinese scholars conducted many experimental studies on the soil erosion forecast model and constructed empirical models of basin erosion and sand production [17,18]. The construction of a soil erosion model effectively reflects the complicated relationship and interaction between soil erosion and influencing factors. In this study, RUSLE was applied for the quantitative calculation of soil erosion intensity. The calculation formula is as follows:

$$A = R \times C \times K \times LS \times P \quad (1)$$

where A is the annual average soil loss (t/(hm^2·a)); R is the rainfall erosivity ((MJ·mm)/(hm^2·h·a)); K is the soil erodibility factor ((t·h)/(MJ·mm)); LS is the landform factor, where L is the slope length factor and S is the slope factor (dimensionless); C is the vegetation cover and management factor (dimensionless); and P is the soil–water conservation measure factor (dimensionless).

(1) Rainfall erosivity factor (R). Rainfall erosivity is the potential ability of rainfall to cause soil erosion. R is a dynamic index for evaluating such an ability, and it is the primary factor in RUSLE. It is expressed as follows [19]:

$$R = 5.249 \left(\sum_{n=1}^{12} \frac{Pi^2}{Pn} \right)^{1.205}, \quad (2)$$

where P_i is the precipitation in the nth month (mm), and P_n is the annual precipitation (mm).

(2) Soil erodibility factor (K). Soil erodibility is an important parameter of soil erosion forecasting and land-use planning. In this study, the K value in the Environmental Policy-integrated Climate model was used to estimate the soil erodibility factor in the RUSLE model [20]. The calculation formula is

$$K = (0.2 + 0.3exp(-0.0256SAN(1 - SIL/100)))\left(\frac{SIL}{CLA+SIL}\right)^{0.3} \left(1 - \frac{0.25C}{C+exp(3.72-2.95C)}\right)\left(1 - \frac{0.7SN_1}{SN_1+exp(-5.51-22.9SN_1)}\right), \quad (3)$$

where SAN, SIL, CLA, and C are the contents of sand, particles, clay particles, and organic carbon (%), SN1 = 1 − SAN/100.

(3) Landform factor (LS).

The calculation of L. In ArcGis10.2, the slope length, λ, is extracted through DEM calculation. The calculation formulas of the slope length factor, proposed by Wischmeier and Smith [21], are as follows:

$$L = (\lambda/22.13)^{\alpha}, \quad (4)$$

$$\alpha = \beta/(\beta + 1), \quad (5)$$

$$\beta = (\sin\beta/0.0896)/(3.0(sin\theta)^{0.8} + 0.56), \quad (6)$$

where λ is the slope length, α refers to the slope length index, the slope length of a standard area is 22.13 (m), and θ is the slope extracted using DEM.

Calculation of slope factor (S). For a gentle slope, the slope formula proposed by McCool et al. was applied. For a steep slope, the formula established by Liu on the Loess Plateau was used [22]:

$$S = 10.8\sin\theta + 0.03 \quad \theta < 5^\circ, \quad (7)$$

$$S = 16.8\sin\theta - 0.50 \quad 5^\circ \leq \theta < 10^\circ, \quad (8)$$

$$S = 21.91\sin\theta - 0.96 \quad \theta \geq 10^\circ, \quad (9)$$

where S is the slope factor, and θ is the slope. According to the above method and formula, the grid factor diagram of LS can be obtained.

(4) Vegetation cover and management factor (C). This factor can inhibit erosion to some extent. The greater its value, the smaller the vegetation effect on erosion reduction. In this study, C was calculated using NDVI, which is based on remote-sensing images [23,24]. The calculation formula is as follows:

$$c = \frac{NDVI - NDVI_{\min}}{NDVImin_{max}}, \tag{10}$$

where NDVI is the normalized difference vegetation index of the calculated pixel. $NDVI_{min}$ refers to the minimum NDVI of the study area, and $NDVI_{max}$ refers to the maximum NDVI.

C was calculated using the revised form of the algorithm proposed by Cai Congfa et al. The algorithm avoids abnormal values (C > 1) when C ranges between 0 and 0.1 [25]. The calculation formula is

$$\mathrm{C} = 1,\ 0 \le c \le 9.6\% \tag{11}$$

$$\mathrm{C} = 0.6508 - 0.3436\mathrm{lgc}\ ,\ 9.6\% < \mathrm{c} \le 78.3\%, \tag{12}$$

$$\mathrm{C} = 0,\ \mathrm{c} > 78.3\%. \tag{13}$$

where lgc denotes the logarithm of c based on 10.

(5) Soil–water conservation measure factor (P). According to existing research results, the present land-use map obtained from remote-sensing interpretation classification was used for the valuation of p [26,27] (Table 1).

Table 1. Land use *p* factor assignment.

Cultivated Land	Forestland	Grassland	Water	Construction Land	Unused Land
0.3	0.2	0.3	0	0	1

2.3.2. Soil Wind Erosion Model

The use of a soil wind erosion model is an important technique for analyzing soil erosion. Among many models, the RWEQ fully considers multiple factors, such as meteorology, soil erodibility, soil crust, surface vegetation cover, and surface roughness. The RWEQ has the advantages of the comprehensive consideration of factors and data accessibility [28–31]. The basic form of the model is as follows:

$$Q_{max}, \tag{14}$$

$$S = 150.71[WF{\cdot}EF{\cdot}SCF{\cdot}K'{\cdot}C]^{-0.3711}, \tag{15}$$

$$S_L = \frac{2z}{S^2}Q - (z/s)2_{max}, \tag{16}$$

where Q_{max} is the maximum throughput of wind-blown sand (kg/m), S is the length of the key plot (m), S_L is the soil wind erosion content of soil ($t{\cdot}hm^{-2}{\cdot}a^{-1}$), z is the calculated downwind distance (m), WF is the meteorological factor (kg/m), EF is the soil erodibility factor, SCF is the soil crust factor, K′ is the surface roughness factor, and COG refers to the vegetation factor. The above parameters are dimensionless.

(1) WF refers to the effects of meteorological factors, such as precipitation, wind velocity, temperature, and snow depth, on soil wind erosion. The formula is

$$WF = \frac{WS{\cdot}N_d{\cdot}\rho}{N{\cdot}g}{\cdot}SW{\cdot}SD, \tag{17}$$

$$SW = \frac{ET_0 - (R + I)\left(\frac{R_d}{N_d}\right)}{ET_0} \quad (18)$$

$$SD = 1 - P(H_{snow} > 25.4 \text{ mm}), \quad (19)$$

where WF is the meteorological factor (kg/m); WS is the wind velocity (m/s^3); N and Nd refer to wind velocity and the number of test days, respectively; ρ is the air density (kg/m^3), g is the gravitational acceleration (m/s^2), SW is the soil moisture factor, and SD is the snow cover factor. These factors are dimensionless. ET_0 is potential relative evaporation (mm), R is rainfall (mm), I is the irrigation amount (mm), R_d is rainfall or irrigation days, N_d is the monthly wind speed greater than 5 m/s, and H_{snow} is the snow depth (mm).

(2) EF and SCF are related to physical and chemical soil properties. They reflect the soil wind erosion content caused by such properties and mechanical composition. The formulas are [32]:

$$WF = \frac{29.09 + 0.31S_a + 0.17S_i + 0.33\frac{S_a}{Cl} - 2.59OM - 0.95CaCO_3}{100}, \quad (20)$$

$$SCF = \frac{1}{1 + 0.0066Cl^2 + 0.021OM^2}, \quad (21)$$

where EF is the soil erodibility and SCF is the soil crust. Sa, Si, Cl, OM, and $CaCO_3$ are the respective contents of coarse sand, silt, clay particle, organic matter, and calcium carbonate in the soil.

K′:

$$K' = cos\alpha, \quad (22)$$

where α is the terrain slope and is extracted using DEM images in ArcGis [33].

Vegetation coverage (COG) has an important influence on soil wind erosion and may hinder soil particles' movement with the wind to some extent.

$$COG = e^{-0.0438c}, \quad (23)$$

where c is the vegetation coverage (%).

3. Results

3.1. Evolutionary Laws of Soil Erosion across 30 Years

The water and wind erosion moduli in Baotou City from 1990 to 2020 were collected based on the RUSLE and RWEQ models (Figure 2). The results indicated that the water erosion modulus first increased before 2000 and then decreased. The water erosion modulus increased from 14.26 $t/hm^2 \cdot a$ in 1990 to 17.37 $t/hm^2 \cdot a$ in 1995. In 2000, the water erosion modulus decreased by 11.92 $t/hm^2 \cdot a$ compared with that in 1995, with great fluctuation in annual changes. However, the water erosion modulus has been continuously increasing since 2005, exhibiting a total increase of 21.4 $t/hm^2 \cdot a$ by 2020. The wind erosion modulus increased from 11.81 $t/hm^2 \cdot a$ in 1990 to 13.22 $t/hm^2 \cdot a$ in 2000. In the 21st century, the wind erosion modulus exhibited a decreasing trend and a total decrease of 4.04 $t/hm^2 \cdot a$ by 2020.

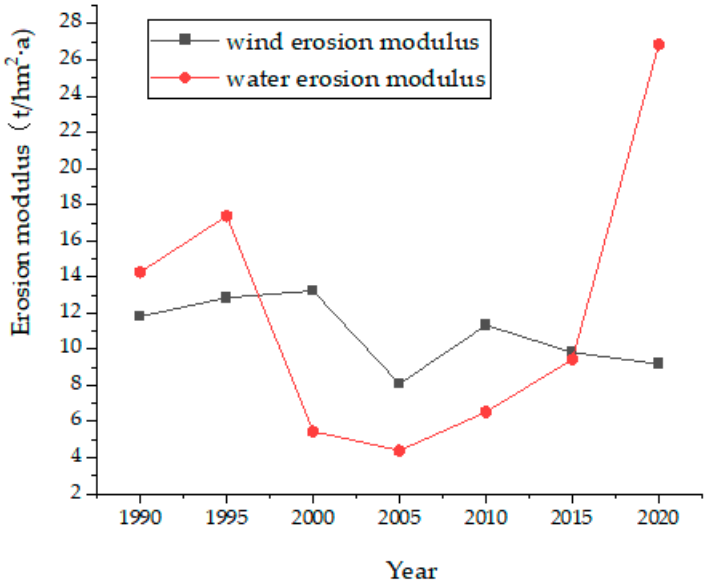

Figure 2. Soil erosion modulus in Baotou City.

According to the Soil Erosion Classification and Grading Standard (SL190-2007) [34], the soil erosion results were classified considering the practical situations in Baotou City (Figure 3). For the quantitative analysis of the mutual transformation laws of soil erosion intensity, and considering the construction of the land-use change diagram [35], the soil erosion grading diagrams for 1990 and 2020 were superposed using GIS and Excel, producing the transfer matrices (Tables 2 and 3) and diagram (Figure 4) of soil erosion intensity. The results indicated that the soil water erosion intensity in an area of 10,241.05 km^2 increased from 1990 to 2020 but decreased in an area of 2456 km^2. The area with decreasing soil wind erosion was 10,928.87 km^2, and the area with increasing soil wind erosion was 128.67 km^2. The area where the soil erosion intensity changed from "light" to "light" was obviously larger than the areas of other transfer types. Light erosion occupied the largest area in Baotou City, and the light erosion condition was relatively stable. Great areas where soil water erosion changed from moderate to high and from light to moderate or high were observed, indicating that soil water erosion intensified gradually in the study area. The soil wind erosion presented the opposite situation, slowly decreasing.

According to the above analysis, the series of recent governing projects in the Yellow River Basin, such as small basin management, soil and water conservation and other regional mountain closure and forest cultivation, farmland return to forest, and strengthened river bank protection and slope protection, can inhibit soil water erosion to some extent. However, serious soil–water loss remains. Soil wind erosion was mitigated, to some extent, because of the Beijing–Tianjin sandstorm source control. The regional wind-proofing and sand-fixing abilities were strengthened, which decreased sandstorm damage to a large extent.

Table 2. Soil water erosion intensity transfer matrix in Baotou City.

1990	2020					
	0–2	2–25	25–50	50–80	80–150	>150
0–2	1384.98	2392.63	705.79	220.44	235.75	167.34
2–25	1673.36	11,929.70	4196.23	549.51	301.36	57.10
25–50	121.74	226.38	420.11	485.48	285.92	60.58
50–80	69.48	49.20	94.56	146.14	329.72	88.30
80–150	49.38	18.70	36.11	39.69	183.34	164.90
>150	26.28	1.36	5.47	9.65	34.64	135.06

The unit of measurement is km^2.

Table 3. Soil wind erosion intensity transfer matrix in Baotou City.

1990	2020					
	0–2	**2–25**	**25–50**	**50–80**	**80–150**	**>150**
0–2	1303.66	58.89	21.12	3.94	1.78	0.00
2–25	3893.86	10,694.30	9.53	0.56	0.48	0.00
25–50	155.70	3724.68	2198.43	16.51	1.30	0.00
50–80	6.58	138.36	1854.36	242.31	9.26	1.06
80–150	11.98	20.43	61.20	1015.92	1908.21	4.24
>150	0.00	0.93	0.52	8.36	35.99	61.75

The unit of measurement is km^2.

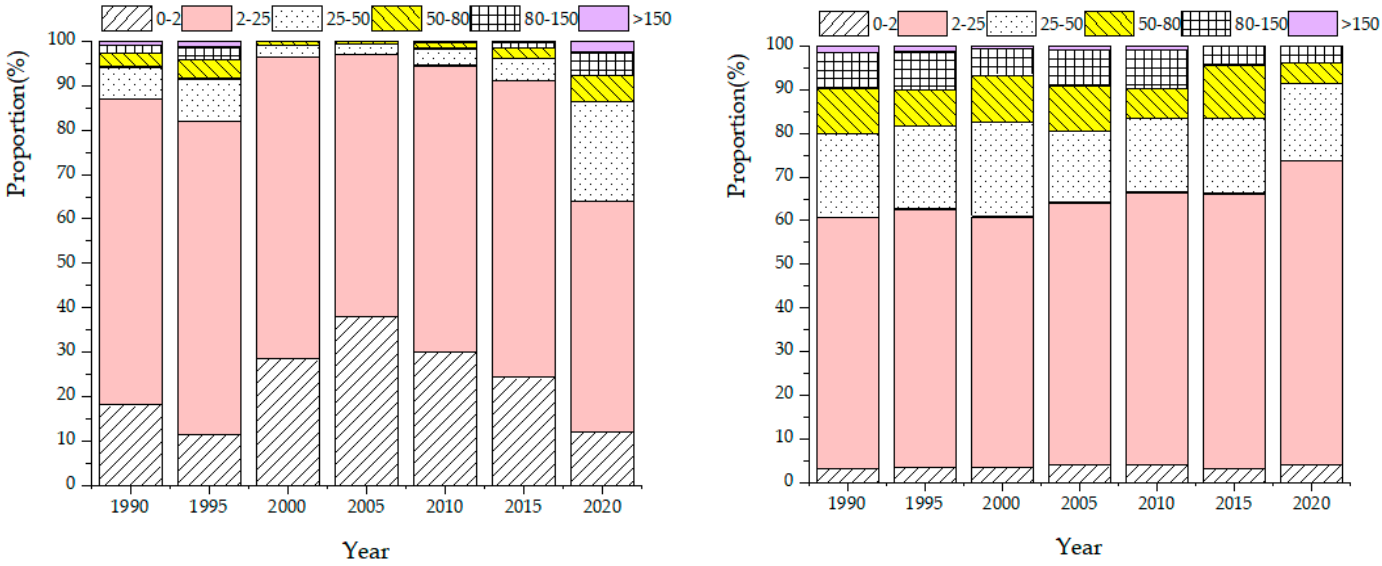

Figure 3. Soil erosion grading map of Baotou City from 1990 to 2020. (**a**) Scale map of soil water erosion grading in Baotou City (%); (**b**) scale map of soil wind erosion grading in Baotou City.

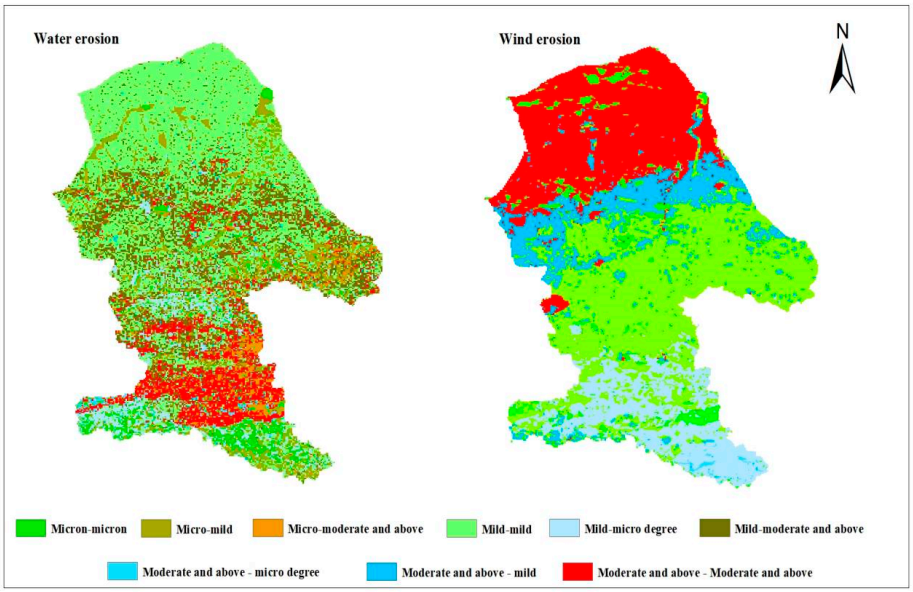

Figure 4. Soil water erosion and soil wind erosion intensity transfer matrices in Baotou City.

3.2. Spatial Evolutionary Laws of Soil Erosion across 30 Years

Since the 1990s, the spatial distribution features of water and wind erosion moduli in Baotou City have generally been kept constant. Specifically, the water erosion modulus presents a rising trend, whereas the wind erosion modulus presents a decreasing trend (Figures 5 and 6).

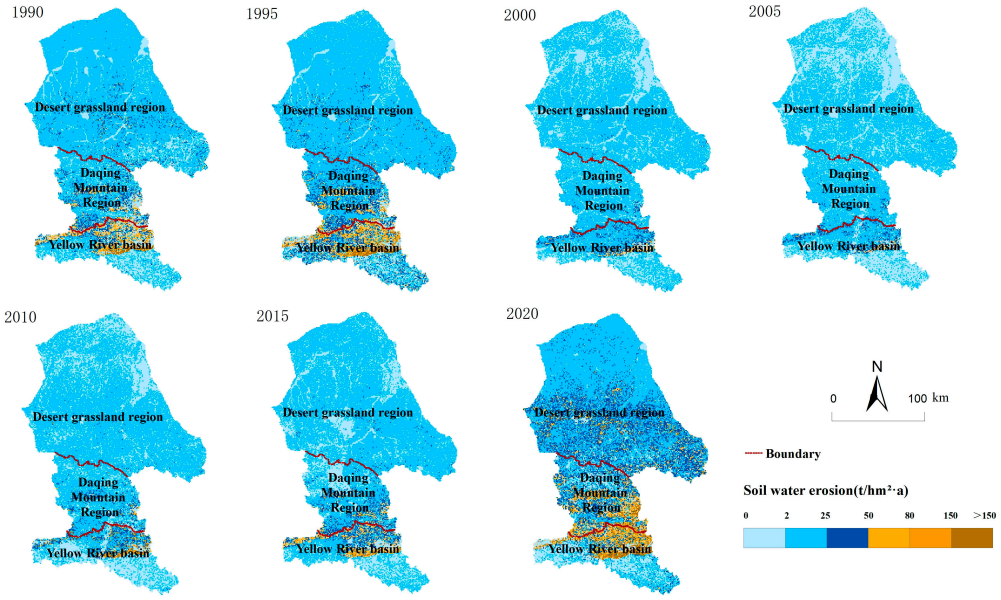

Figure 5. Spatial distribution of soil water erosion in Baotou City.

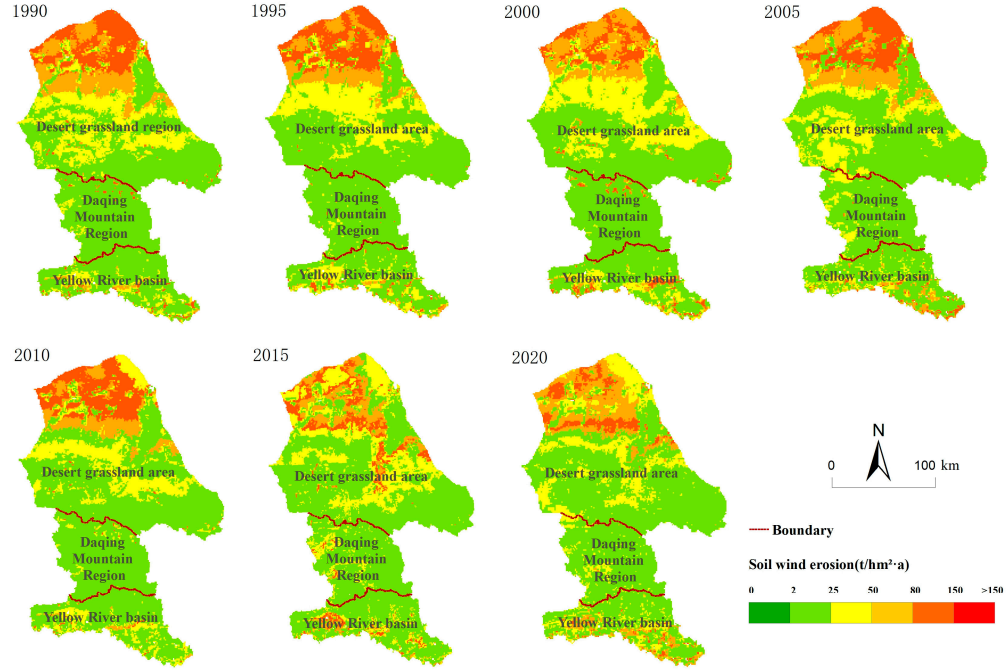

Figure 6. Spatial distribution of soil wind erosion in Baotou City.

Soil water erosion was extensively distributed across Baotou City from 1990 to 2020. The degree of soil water erosion was low, and soil water erosion was mainly of mild and light types, which accounted for more than 80% of erosion. In terms of spatial changes, the soil water erosion content in the Yellow River Basin in the south increased significantly in the 1990s. Before 2015, the soil water erosion intensity in Baotou City declined dramatically

compared with that in the 1990s, indicating that soil water erosion was effectively inhibited. In 2020, soil water erosion was relatively serious. The area with mild and light erosion accounted for less than 65% of the total area, and the soil water erosion intensity changed to moderate or high. Moreover, the soil water erosion area in the desert grassland region increased by 4840.5 km^2, and the soil water erosion area in the Yellow River Basin decreased by 1300.5 km^2 compared with those in 1990. In view of the spatial distribution, regions with great wind erosion moduli decreased in the study area, whereas those with small wind erosion moduli continuously increased. In general, the wind erosion modulus of the study area presented a decreasing trend. The area with at least a moderate wind erosion modulus decreased by 11.14 t/hm^2, and the soil wind erosion intensity changed to mild and light degrees. In terms of spatial changes, the soil wind erosion intensity of the desert grassland decreased. Owing to some artificial interventions, such as rotational grazing, grazing rest, and enclosed grazing, soil wind erosion was greatly mitigated. The spatial changes of the central Daqing Mountain Region and the Yellow River Basin were not obvious, and light soil wind erosion played a dominant role.

Influenced by man-made interferences (grazing), the vegetation coverage in the desert grassland north of Baotou City was relatively poor. The vegetation coverage in the middle and southern regions was relatively good, which was attributed to artificial intervention and ecological restoration and protection, such as small basin engineering construction, urban soil–water conservation, and ecological construction. Moreover, serious soil wind erosion and soil water erosion were recorded, respectively, in the north and south, which were related to the comprehensive influences of rainfall climate, soil, and terrain. The wind erosion moduli in the local areas of the Yellow River Basin were relatively high. The soil–water loss, under the cumulative effect of soil wind erosion and soil water erosion, not only brought serious damage to the ecological environment but also increased the sediments in the Yellow River Basin.

3.3. Potential Driving Factors of Soil Erosion Changes

3.3.1. Meteorological Factors

Baotou City is upstream of the Yellow River and is in grassland in the north. Influenced by nature and human activities, this city exhibits serious grassland degradation, desertification, and salinization. The productivity and biodiversity of the natural grassland in the moderate and severe degradation regions decreased [36]. Given the seasonally dry climate conditions, Baotou City presents relatively low annual precipitation, weak stability of the forest ecosystem, and a vulnerable ecological background [36]. Soil erosion is influenced by natural factors (e.g., climate, vegetation type, terrain, and soil features) and man-made factors (e.g., land use). Meteorological factors and vegetation exhibit great changes. Climate changes can influence the soil erosion intensity by changing precipitation and wind velocity, including their strength and spatial distribution [37,38].

The mean annual precipitation in Baotou City during the 1990–2020 period was 176.40 mm. Figure 7a shows that the precipitation had a significantly positive correlation with the water erosion modulus ($R^2 = 0.93$, $p < 0.001$). That is, soil water erosion increased with precipitation. Wind velocity is the primary meteorological factor that influences soil wind erosion, and wind is the most direct power source of soil wind erosion. The average annual wind speed in Baotou City from 1990 to 2020 was 2.41 m/s. Figure 7b illustrates that wind velocity was positively related to the wind erosion modulus ($R^2 = 0.81$, $p < 0.001$). The greater the wind velocity, the higher the soil wind erosion intensity.

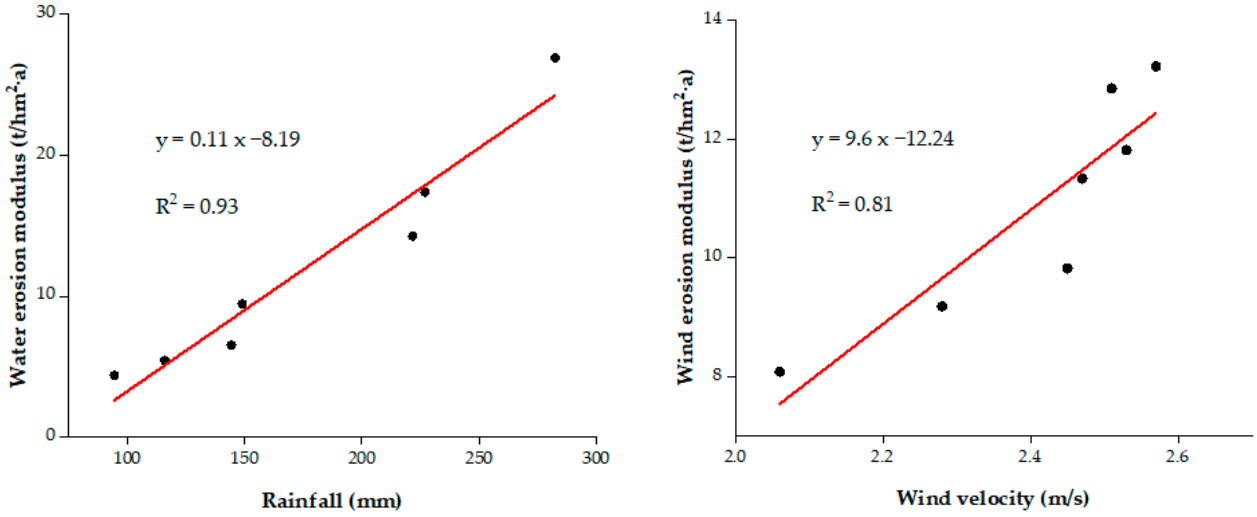

(**a**) (**b**)

Figure 7. Relationship between soil erosion and meteorological factors in Baotou City. (**a**) Relationship between water erosion modulus and precipitation; (**b**) relationship between wind erosion modulus and wind velocity.

3.3.2. Vegetation Pattern Evolution

Surface vegetation can inhibit soil erosion to some extent. Vegetation coverage is one of the important primary factors that inhibit soil water erosion, sediment loss, soil wind erosion, and dust emission. Vegetation coverage is also a sensitive factor that influences soil erosion. Its changes may cause changes in soil erosion. The underground part of vegetation not only strengthens soil stability but also decreases the influence of runoff washing. The aboveground part of plants can decrease the eroding force of precipitation. Figure 8 depicts that the vegetation coverage in Baotou City decreased at first and has increased in recent years. The vegetation coverage decreased from 1990 to 1995, which was mainly related to excessive reclamation and grazing. Grassland degradation was serious. Vegetation coverage from 1995 to 2005 increased dramatically, which was mainly related to the implementation of farmland return to forest and grassland. Grassland and forest ecosystems were stable. The vegetation coverage from 2005 to 2020 fluctuated as a result of the influences of meteorological factors. Low precipitation, low temperature, and poor grass productivity were observed. Influenced by unreasonable utilization, serious grassland degradation and wind erosion-induced desertification occurred. The degraded grassland accounted for more than 70% of the total grassland. Moreover, rat and insect diseases occurred frequently in the grassland, which seriously damaged the vegetation.

To quantify the influences of meteorological factors and vegetation coverage on soil erosion, soil water erosion and soil wind erosion equations were constructed:

$$Y_1 = 0.114X_{\text{rainfall}} + 12.920 \times {}_2 - 13.030 \qquad (R^2 = 0.94), \tag{24}$$

$$Y_2 = 6.056X_{\text{wind velocity}} - 10.920 \times {}_2 + 0.554 \qquad (R^2 = 0.894), \tag{25}$$

where Y_1 represents the water erosion modulus and Y_2 represents the wind erosion modulus (t/(hm^2·a). X_{rainfall} refers to precipitation (mm), and $X_{\text{wind velocity}}$ denotes wind velocity (m/s). X_2 is the vegetation coverage. According to the results, global warming and drought caused by climate changes can change the physical and chemical properties of soil and vegetation coverage, thus indirectly influencing soil erosion (<0.005) [39].

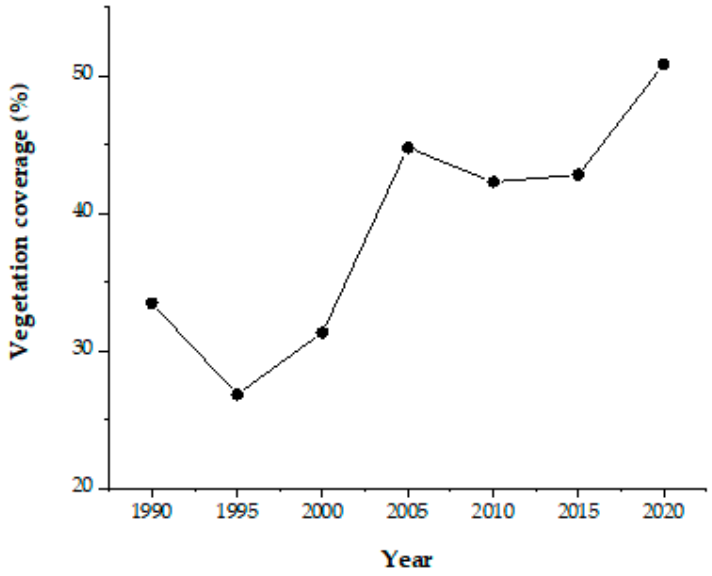

Figure 8. Vegetation coverage in Baotou City from 1990 to 2020.

3.3.3. Ecological Restoration Project

The land-use types in Baotou City during the 1990–2020 period were mainly characterized by increasing forestland; urban expansion; and decreased grassland, water, and unused land (Table 4 and Figure 9). The areas of different land-use types slightly but frequently changed. Cultivated land was mainly transformed into forestland, grassland, and construction land. The Daqing–Wula Mountains are an important component of the biodiversity priority area in the west Erdos–Yin Mountain–Helan Mountain in China. Recently, Baotou City has vigorously carried out natural forest protection and ecological noncommercial forest construction projects. The total forestland area in Baotou City was 224,328.62 ha by 2020, accounting for 8.16% of the total territorial area of the city. According to the statistics in the Forest Department [36], forest coverage increased to 18.3%. Specifically, the most extensive distributions of forest resources were recorded in Tuyouqi, Guyang County, and the Shiguai District.

Table 4. Land-use transfer matrix in Baotou City during the 1990–2020 period.

1990	2020					
	Cultivated Land	**Woodland**	**Grassland**	**Water**	**Construction Land**	**Unutilized Land**
Cultivated land	3528.63	92.74	1266.48	9.41	180.32	3.17
Woodland	97.13	0.89	7.35	0.28	3.63	0.00
Grassland	1788.42	2587.04	14,801.99	58.67	652.35	929.15
Water	106.77	74.37	752.66	88.26	12.05	40.03
Construction land	104.73	129.22	55.34	9.91	117.16	1.42
Unutilized land	63.04	39.49	57.09	3.22	41.07	9.55

The unit of measurement is hm^2.

The grassland in the northern area of Baotou City is mainly desert grassland and steppe desert, accounting for 50% of the grassland area in Baotou City. Soil erosion is more serious because of the following two reasons. On one hand, noncontrollable factors, such as climate change, strong rainfall, and drought response, can result in soil erosion to some extent. On the other hand, human activities, such as mining, influence vegetation coverage, especially open pit mines. By 2020, the mining land area in Baotou City was 31,277.67 ha, accounting for 1.13% of its total area. Although ecological restoration in mines has been facilitated continuously for years, waste mining areas remained (6054.53 ha) [36], causing damage to the ecological environment and intensifying soil erosion. The imbalance

between grassland productivity and animal husbandry production led to nutrient loss in the grassland ecosystem and intensified grassland degradation. According to the national key ecological function zoning, the northern region of Baotou City is not only the core area of the grassland ecological function zone at the northern foot of the Yin Mountain but also an important component of the wind erosion prevention and sand fixation belt in Northern China. A warm dry steppe belt is located south of the Yin mountain, and a mesotemperature steppe belt is located north of the Yin Mountain. With the recent implementation of policies and systems—such as Beijing–Tianjin sandstorm resource control, farmland return to forest, grazing prohibition, grazing rest, and rotational grazing—including rewards and subsidies for grasslands, the general worsening trend of the grassland ecological environment in Baotou City was inhibited. Specifically, the comprehensive vegetation coverage increased to 36.58%. The grassland ecosystem functions improved. Wind erosion prevention and sand fixation, biodiversity maintenance, and soil–water conservation ecological service functions were guaranteed.

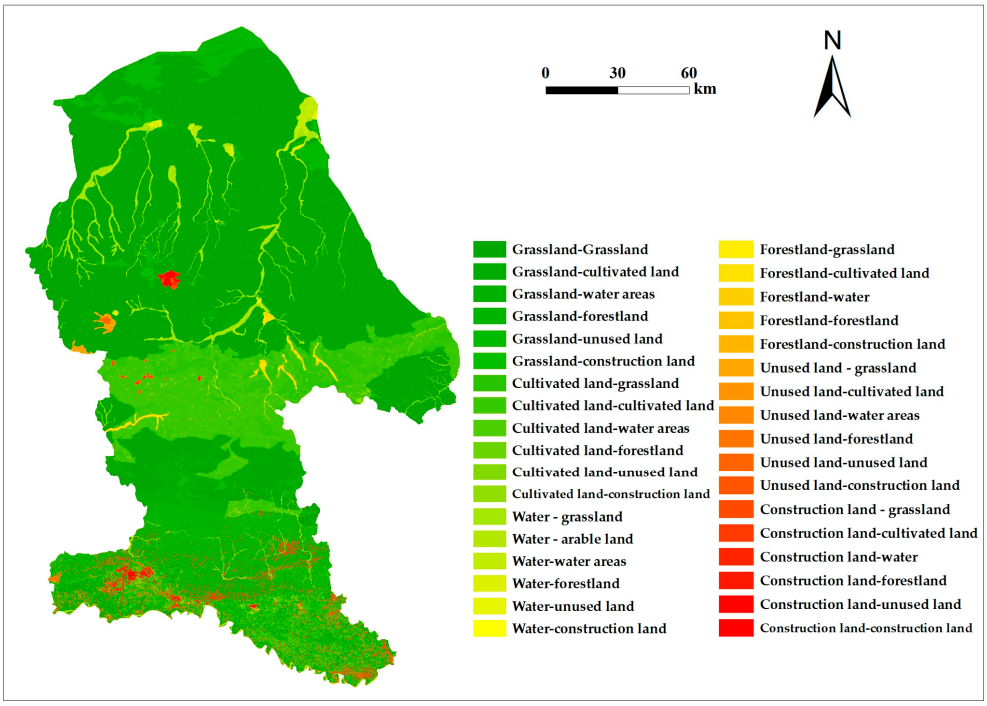

Figure 9. Land-use transfer matrix for Baotou City during the 1990–2020 period.

4. Discussion

Soil erosion is a complicated process. Soil erosion intensity changes are the cumulative results of different factors. Meteorological factors, soil type, landform, and vegetation coverage influence the differences in soil erosion changes [40]. Meteorological factors are primary factors that influence soil erosion. Some studies have reported that rainfall is the direct controlling factor of soil water erosion and the kinetic energy of precipitation acts on the soil. The impact of raindrops on bare soil destroys the soil structure, resulting in infiltration capacity loss that intensifies surface runoff and soil erosion. Wind velocity is the dominant factor influencing soil wind erosion. When the wind velocity exceeds the minimum tolerance of sands, surface soil particles are removed from the land surface [41]. Soil erosion content is estimated through model inversion. Soil erosion results are quickly obtained based on climate, vegetation coverage, and land use and have been widely applied in studies concerning soil erosion. The RUSLE and the RWEQ have been extensively used in China and foreign countries. Bufalini, Scheper, et al. [42–46] verified a soil erosion model using practical data and verified the accuracy of the results. The soil factor is an index for evaluating soil erosion and soil–water loss. Soil properties are mainly sensitive to soil water

content, biological effects, and climatic disturbances. The soil properties in different areas of the same region vary [47]. Land use is an important factor affecting soil erosion. From the model point of view, when land use changes, vegetation factors and soil and water conservation measures also change, so land-use changes may affect soil erosion changes. Although the results are different from the actual erosion modulus in a specific time and region, this study has certain credibility in simulating the spatiotemporal changes of the soil erosion modulus. In a similar fashion, soil water content and vegetation cover influence the susceptibility of soils to wind erosion. Soil moisture contents as low as 5% by weight add cohesive strength to soils and make them more resistant to wind erosion. A vegetation cover contributes to reducing soil erosion in several ways: the vegetation canopy creates a "dead air" zone near the ground surface that prevents deflation by the wind and the root mass contributes to the overall strength of the soil, thus reducing the capacity for wind erosion.

Land-use and land-cover changes are not only important for studying global environmental changes but also clearly reflect the close relationships between human activities and the natural environment [48–50]. Baotou is a grassland city based on industrial development and comprises various ecosystems, including the grassland ecosystem centered at Damaoqi, the forest ecosystem centered at the Daqing–Wula Mountains, and the wetland ecosystem centered at the Yellow River Wetland Park (Figure 10). In the most recent 30 years, Baotou City has implemented various ecological projects according to different ecosystems. To address grassland degradation and desertification, the focus must be on restoring degraded grassland; curbing grassland reclamation; and returning low-quality farmland to grassland, especially implementing grazing prohibition, grazing rest, and rotational grazing to strike a balance between forage and animal production. Moreover, grassland protection and desertification control have been strengthened, and grassland quality and ecosystem stability have been improved. Ecological restoration and protection projects have been implemented at the south and north feet of the Daqing Mountain, including the overall planning and implementation of the Beijing–Tianjin sandstorm resource control, natural forest protection, soil–water conservation, farmland return to forest, and other key ecological governance projects, thus strengthening forest resource protection, improving forest quality, and increasing forest ecosystem structure integrity. It strengthened the protective belt construction in watercourse buffer zones along the Yellow River Basin, increased ecological water compensation (ecological water replenishment is an important means of achieving the comprehensive improvement of river channels and an important way to ensure the water use of the ecological environment.), and decreased the soil–water loss and the sediment entrance into the Yellow River. It solves the shortage of water resources in the regional ecosystem and the dynamic balance of the ecological environment by replenishing the damaged ecosystem that cannot meet the ecological water demand. Constructing soil–water conservation engineering and wind prevention–sand fixation systems can effectively decrease man-made soil–water loss. The regional wind erosion prevention and sand fixation ability has been strengthened, land productivity has increased, and the local natural ecological structure has significantly improved.

However, the influence of wind–water composite erosion on the study area remains significant. Industrial and mining developments have destroyed the local ecological environment, thus decreasing the local ecological quality and increasing soil wind erosion and soil water erosion. Hence, in accordance with the importance of ecosystem service functions, ecosystem vulnerability, ecological safety patterns, and ecological problems in Baotou City—and follow the concept of "mountain, water, forest, farmland, lake, and grass" living community—Baotou City further reinforced the wind erosion prevention and sand fixation ecological barrier in the northern grassland, as well as the Daqing–Wula Mountain ecological barrier, to strengthen important ecological safety barriers. Ecological security patterns can solve many problems, such as protecting and restoring biodiversity, maintaining the integrity of the ecosystem structure and processes, realizing effective control, and the continuous improvement of regional ecological environment problems.

These actions also improved ecosystem service functions in Northern China. Moreover, the ecological protection and restoration belt along the Yellow River has been improved. A scientific configuration of protection and repair, such as the introduction of the Yellow River Protection Law in 2022, natural and artificial ecologies, biology, and engineering, have also been implemented. These measures can promote integrated ecological protection and restoration.

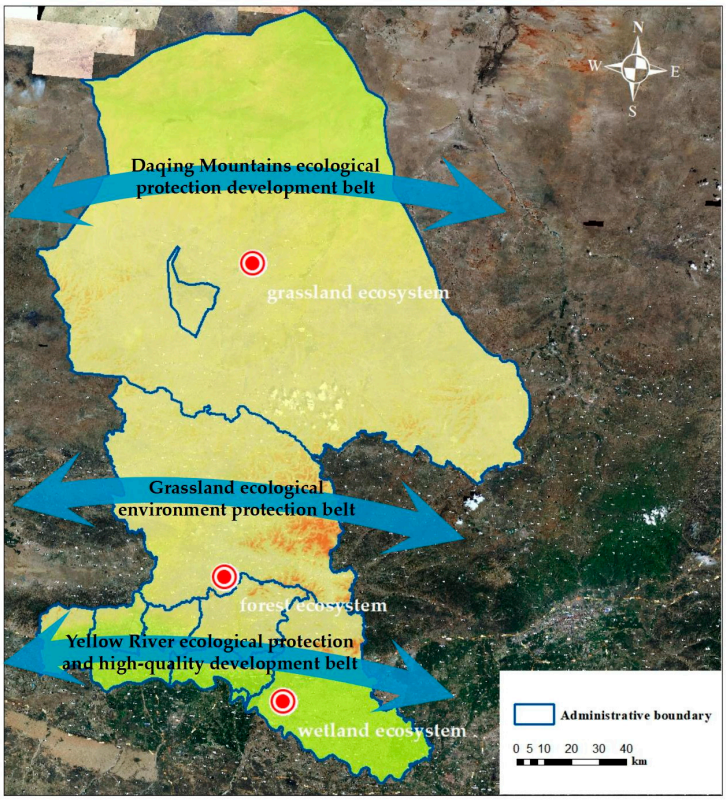

Figure 10. Ecological environmental protection and development in Baotou city.

5. Conclusions

In this study, the spatiotemporal distribution pattern of soil erosion in Baotou City, Inner Mongolia during the 1990–2020 period and its influencing factors were analyzed using GIS technology on the basis of the RUSLE and RWEQ models:

(1) From 1990 to 2020, the water erosion modulus in Baotou City increased first, decreased, and then finally increased, with great fluctuations in annual changes. Specifically, soil water erosion increased continuously from 1990 to 1995 but decreased dramatically from 1995 to 2000 and finally achieved a significant growth trend from 2000 to 2020. The wind erosion modulus in Baotou City continuously decreased, with a small fluctuation in annual changes.

(2) During the study period, the soil water erosion in an area of 10,241.05 hm^2 was intensified, whereas the soil water erosion in an area of 10,241.05 hm^2 was relieved. The area with decreased soil wind erosion was 10,928.87 km^2, and the area with increased soil wind erosion was 128.67 km^2. In terms of spatial changes, the soil water erosion intensity in the entire city decreased significantly compared with levels in the 1990s, indicating that soil water erosion was effectively inhibited. However, soil water erosion was relatively serious in 2020. The area with soil water erosion increased by 4840.5 km^2 in the desert grassland region but decreased by 1300.5 km^2 in the Yellow River Basin. In the study area, the region with a great wind erosion modulus decreased gradually, whereas the area with a small wind erosion modulus continuously increased. However, the area with soil wind erosion generally presented

a decreasing trend. The soil wind erosion intensity in desert grassland declined greatly, indicating that soil wind erosion had significantly improved. The spatial changes in the Daqing Mountain and the Yellow River Basin areas were not obvious, and light wind erosion was dominant.

(3) Meteorological factors are the primary factors that influence soil water erosion and soil wind erosion. Precipitation had a significant correlation with the water erosion modulus ($p < 0.001$), and wind velocity was positively related to the wind erosion modulus ($p < 0.001$). Vegetation coverage is one of the important factors that inhibit soil water erosion, sediment loss, soil wind erosion, and dust emission. Adverse climate changes can influence soil erosion by changing physical and chemical soil properties and vegetation coverage ($p < 0.005$). Baotou City has achieved some successes in mitigating soil erosion and strengthening soil–water conservation. Land-use changes, such as farmland return to forest and grassland and urban expansion, can inhibit the occurrence of soil erosion to some extent. These changes play a crucial role in improving ecological environmental restoration in Baotou City.

Author Contributions: Data processing, writing—original draft preparation, and editing, T.T. and Z.Y.; manuscript validation and revision, J.G.; project administration and funding acquisition, T.Z.; data collection, Z.W. and P.M.; T.T. and Z.Y. are co-first authors. All authors have read and agreed to the published version of the manuscript.

Funding: This study was supported by the Major Science and Technology Projects of the Inner Mongolia Autonomous Region (2021ZD0008), the "Science for a Better Development of Inner Mongolia" program (KJXM-EEDS-2020005) of the Bureau of Science and Technology of the Inner Mongolia Autonomous Region, and the Major Science and Technology Projects of the Inner Mongolia Autonomous Region (2020ZD0009).

Institutional Review Board Statement: Not applicable.

Informed Consent Statement: Not applicable.

Data Availability Statement: The remote sensing images were obtained from the geospatial data cloud (http://www.gscloud.cn/, accessed on 17 December 2022). The meteorological data were taken from the National Data Center for Earth System Science and the National Platform for Basic Conditions of Science and Technology (http://www.geodata.cn, accessed on 17 December 2022). The soil data and snow depth were derived from National Tibetan Plateau Scientific Data (https://data.tpdc.ac.cn, accessed on 17 December 2022).

Acknowledgments: We would like to thank all the partners involved in this study and the experimental platform provided by the Yinshanbeilu National Field Research Station of the Steppe Eco-hydrological System. The authors would like to thank the reviewers for the helpful and constructive comments and suggestions that have substantially improved the quality of this manuscript.

Conflicts of Interest: The authors declare no conflict of interest.

References

1. Batista, P.V.; Davies, J.; Silva, M.L.; Quinton, J.N. On the evaluation of soil erosion models: Are we doing enough? *Earth Sci. Rev.* **2019**, *197*, 102898. [CrossRef]
2. Kumar, R.; Deshmukh, B.; Kumar, A. Using Google Earth Engine and GIS for basin scale soil erosion risk assessment: A case study of Chambal river basin, central India. *J. Earth Syst. Sci.* **2022**, *131*, 228. [CrossRef]
3. Pan, L.D.; Li, R.; Shu, D.C.; Zhao, L.N.; Chen, M.; Jing, J. Effects of rainfall and rocky desertification on soil erosion in karst area of Southwest China. *J. Mt. Sci.* **2022**, *19*, 3118–3130. [CrossRef]
4. Wang, W.; Li, Z.; Yang, R.; Wang, T.; Li, P. Experimental Study of Freeze-Thaw/Water Compound Erosion and Hydraulic Conditions as Affected by Thawed Depth on Loessal Slope. *Front. Environ. Sci.* **2020**, *8*, 609594. [CrossRef]
5. Chappell, A.; Baldock, J.; Sanderman, J. The global significance of omitting soil erosion from soil organic carbon cycling schemes. *Nat. Clim. Chang.* **2016**, *6*, 187–191. [CrossRef]
6. Stefanidis, S.; Alexandridis, V.; Chatzichristaki, C.; Stefanidis, P. Assessing Soil Loss by Water Erosion in a Typical Mediterranean Ecosystem of Northern Greece under Current and Future Rainfall Erosivity. *Water* **2021**, *13*, 2002. [CrossRef]
7. Pretty, J.; Benton, T.G.; Bharucha, Z.P.; Dicks, L.; Flora, C.; Godfray, C.; Goulson, D.; Hartley, S.; Lampkin, N.; Morris, C.; et al. Global assessment of agricultural system redesign for sustainable intensification. *Nat. Sustain.* **2018**, *1*, 441–446. [CrossRef]

8. Nagendra, H.; Bai, X.M.; Brondizio, E.S.; Lwasa, S. The urban south and the predicament of global sustainability. *Nat. Sustain.* **2018**, *1*, 341–349. [CrossRef]
9. Jiang, C.; Zhang, H.Y.; Zhang, Z.D.; Wang, D.W. Model-based assessment soil loss by wind and water erosion in China's Loess Plateau: Dynamic change, conservation effectiveness, and strategies for sustainable restoration. *Glob. Planet. Chang.* **2019**, *172*, 396–413. [CrossRef]
10. Ye, D.; Chou, J.; Liu, J.; Zhang, Z.; Wang, Y.; Zhou, Z.; Ju, H.; Huang, Q. The causes and control measures of sand and dust weather in North China. *Acta Geogr. Sin.* **2000**, *55*, 513–521.
11. Visser, S.M.; Sterk, G.; Ribolzi, O. Techniques for simultaneous quantification of wind and water erosion in semi-arid regions. *J. Arid. Environ.* **2004**, *59*, 699–717. [CrossRef]
12. Yang, C.; Zhen, B.; Zhang, P.; Xiao, P. Analysis on Composite Erosion Process Based on Multi Dynamic Erosion Environment Simulation. *IOP Conf. Ser. Earth Environ. Sci.* **2020**, *526*, 12–25. [CrossRef]
13. Wang, T.; Qu, J.J.; Yao, Z.Y.; Zhang, W.M.; Tuo, W.Q.; Zhang, J.G.; Yang, G.S.; Chen, G.T. The present situation of soil and water loss and comprehensive control countermeasures in the wind-water erosion composite area of the northern agro-pastoral ecotone. *China Soil Water Conserv. Sci.* **2008**, *1*, 28–36+42.
14. He, Z.; He, J. Remote sensing monitoring of the spatiotemporal evolution of vegetation coverage in the Yellow River Basin in the past 32 years. *J. Agric. Mach.* **2017**, *48*, 179–185.
15. Zhu, T.X. Gully and tunnel erosion in the hilly Loess Plateau region, China. *Geomorphology* **2012**, *153–154*, 144–155. [CrossRef]
16. Bullock, A.; King, B. Evaluating China's slope land conversion program as sustainable management in Tianquan and Wuqi counties. *J. Environ. Manag.* **2011**, *92*, 1916–1922. [CrossRef]
17. Liu, B.Y.; Nearing, M.A.; Shi, P.J.; Jia, Z.W. Slope Length Effects on Soil Loss for Steep Slopes. *Soil Sci. Soc. Am. J.* **2000**, *64*, 1759–1763. [CrossRef]
18. Xu, E.Q.; Zhang, H.Q. Change pathway and intersection of rainfall, soil, and land use influencing water-related soil erosion. *Ecol. Indic.* **2020**, *113*, 106281. [CrossRef]
19. Zhang, S.; Xiong, D.H.; Wu, H.; Yuan, Y.; Li, W.X.; Zhang, W.D. Spatial differentiation characteristics of soil erosion in Sunshui River Basin based on RUSLE model. *J. Soil Water Conserv.* **2021**, *35*, 24–30.
20. Gao, H.D.; Li, Z.B.; Jia, L.L.; Li, P.; Xu, G.C.; Ren, Z.P.; Pang, G.W.; Zhao, B.H. Capacity of soil loss control in the Loess Plateau based on soil erosion control degree. *J. Geogr. Sci.* **2016**, *26*, 457–472. [CrossRef]
21. Bufalini, M.; Materazzi, M.; Martinello, C.; Rotigliano, E.; Pambianchi, G.; Tromboni, M.; Paniccià, M. Soil Erosion and Deposition Rate Inside an Artificial Reservoir in Central Italy: Bathymetry versus RUSLE and Morphometry. *Land* **2022**, *11*, 1924. [CrossRef]
22. McCool, D.K.; Foster, G.R.; Mutchler, C.K.; Meyer, L.D. Revised Slope Length Factor for the Universal Soil Loss Equation. *Trans. ASAE* **1989**, *32*, 5. [CrossRef]
23. Gillies, R.R.; Kustas, W.P.; Humes, K.S. A verification of the "triangle" method for obtaining surface soil water content and energy fluxes from remote measurements of the normalized difference vegetation index (NDVI) and surface. *Int. J. Remote Sens.* **1997**, *18*, 3145–3166. [CrossRef]
24. Panagos, P.; Borrelli, P.; Meusburger, K.; Alewell, C.; Lugato, E.; Montanarella, L. Estimating the soil erosion cover-management factor at the European scale. *Land Use Policy* **2015**, *48*, 38–50. [CrossRef]
25. Cai, C.F.; Ding, S.W.; Shi, Z.H.; Huang, L.; Zhang, G.Y. Study of applying USLE and geographical information system IDRISI to predict soil erosion in small watershed. *J. Soil Water Conserv.* **2000**, *14*, 19–24.
26. Panagos, P.; Borrelli, P.; Meusburger, K.; van der Zanden, E.H.; Poesen, J.; Alewell, C. Modelling the effect of support practices (P-factor) on the reduction of soil erosion by water at European scale. *Environ. Sci. Policy* **2015**, *51*, 23–34. [CrossRef]
27. Ochoa-Cueva, P.; Fries, A.; Montesinos, P.; Rodríguez-Díaz, J.A.; Boll, J. Spatial estimation of soil erosion risk by land-cover change in the Andes of southern Ecuador. *Land Degrad. Dev.* **2015**, *26*, 565–573. [CrossRef]
28. Buschiazzo, D.E.; Zobeck, T.M. Validation of WEQ, RWEQ and WEPS wind erosion for different arable land management systems in the Argentinean Pampas. *Earth Surf. Process. Landf.* **2008**, *33*, 1839–1850. [CrossRef]
29. Jiang, N.; Zhang, Q.; Zhang, S.; Zhao, X.; Cheng, H. Spatial and temporal evolutions of vegetation coverage in the Tarim River Basin and their responses to phenology. *Catena* **2022**, *217*, 106489. [CrossRef]
30. Zhang, H.; Fan, J.; Cao, W.; Harris, W.; Li, Y.; Chi, W.; Wang, S. Response of wind erosion dynamics to climate change and human activity in Inner Mongolia, China during 1990 to 2015. *Sci. Total Environ.* **2018**, *639*, 1038–1050. [CrossRef]
31. Li, J.; Ma, X.; Zhang, C. Predicting the spatiotemporal variation in soil wind erosion across Central Asia in response to climate change in the 21st century. *Sci. Total Environ.* **2020**, *709*, 136060. [CrossRef]
32. Fryrear, D.; Krammes, C.; Williamson, D.; Zobeck, T. Computing the wind erodible fraction of soils. *J. Soil Water Conserv.* **1994**, *49*, 183.
33. Shen, L.; Tian, M.R.; Gao, J.X. Analysis of soil wind erosion and main influencing factors in Hunshandake desertification control ecological function area based on RWEQ model. *J. Soil Water Conserv. Res.* **2016**, *23*, 90–97.
34. Ministry of Water Resources of the People's Republic of China. Available online: http://www.mwr.gov.cn/ (accessed on 12 February 2023).
35. Liu, Y.; Hou, X.; Qiao, J.; Zhang, W.; Fang, M.; Lin, M. Evaluation of soil erosion rates in the hilly-gully region of the Loess Plateau in China in the past 60 years using global fallout plutonium. *Catena* **2023**, *220*, 106666. [CrossRef]

36. Baotou Forestry and Grassland Bureau. *Baotou Forestry and Grassland Bureau Development '14th Five-Year' Plan*; EB/OL.2021; Baotou Forestry and Grassland Bureau: Baotou, China, 2021.
37. Fenta, A.A.; Tsunekawa, A.; Haregeweyn, N.; Poesen, J.; Tsubo, M.; Borrelli, P.; Panagos, P.; Vanmaercke, M.; Broeckx, J.; Yasuda, H.; et al. Land susceptibility to water and wind erosion risks in the East Africa region. *Sci. Total Environ.* **2020**, *703*, 135016. [CrossRef]
38. Borrelli, P.; Panagos, P.; Ballabio, C.; Lugato, E.; Weynants, M.; Montanarella, L. Towards a Pan-European assessment of land susceptibility to wind erosion. *Land Degrad. Dev.* **2016**, *27*, 1093–1105. [CrossRef]
39. Qian, K.; Ma, X.; Wang, Y.; Yuan, X.; Yan, W.; Liu, Y.; Yang, X.; Li, J. Effects of Vegetation Change on Soil Erosion by Water in Major Basins, Central Asia. *Remote Sens.* **2022**, *14*, 5507. [CrossRef]
40. Chen, C.; Zhao, G.; Zhang, Y.; Bai, Y.; Tian, P.; Mu, X.; Tian, X. Linkages between soil erosion and long-term changes of landscape pattern in a small watershed on the Chinese Loess Plateau. *Catena* **2023**, *220*, 106659. [CrossRef]
41. Borrelli, P.; Lugato, E.; Montanarella, L.; Panagos, P. A new assessment of soil loss due to wind erosion in european agricultural soils using a quantitative spatially distributed modelling approach. *Land Degrad. Dev.* **2016**, *28*, 335–344. [CrossRef]
42. Du, H.Q.; Wang, T.; Xue, X.; Li, S. Estimation of soil organic carbon, nitrogen, and phosphorus losses induced by wind erosion in Northern China. *Land Degrad. Dev.* **2019**, *30*, 1006–1022. [CrossRef]
43. Zou, X.; Li, H.; Kang, L.; Zhang, C.; Jia, W.; Gao, Y.; Zhang, J.; Yang, Z.; Zhang, M.; Xu, J.; et al. Soil wind erosion rate on rough surfaces: A dynamical model derived from an invariant pattern of the shear-stress probability density function of the soil surface. *Catena* **2022**, *219*, 106633. [CrossRef]
44. Alizadeh, M.; Zabihi, H.; Wolf, I.D.; Langat, P.K.; Pour, A.B.; Ahmad, A. Remote sensing technique and ICONA based-GIS mapping for assessing the risk of soil erosion: A case of the Rudbar Basin, Iran. *Environ. Earth Sci.* **2022**, *81*, 512. [CrossRef]
45. Zhao, C.; Zhang, H.; Wang, M.; Jiang, H.; Peng, J.; Wang, Y. Impacts of climate change on wind erosion in Southern Africa between 1991 and 2015. *Land Degrad. Dev.* **2021**, *32*, 2169–2182. [CrossRef]
46. Scheper, S.; Weninger, T.; Kitzler, B.; Lackóová, L.; Cornelis, W.; Strauss, P.; Michel, K. Comparison of the spatial wind erosion patterns of erosion risk mapping and quantitative modeling in Eastern Austria. *Land* **2021**, *10*, 974. [CrossRef]
47. Li, J.; Chen, H.; Zhang, C. Impacts of climate change on key soil ecosystem services and interactions in Central Asia. *Ecol. Indic.* **2020**, *116*, 106490. [CrossRef]
48. Wu, J.; Zheng, X.; Zhao, L.; Fan, J.; Liu, J. Effects of Ecological Programs and Other Factors on Soil Wind Erosion between 1981–2020. *Remote Sens.* **2022**, *14*, 5322. [CrossRef]
49. Gao, G.L.; Yin, X.L.; Ding, G.D.; Zhao, Y.Y.; Sun, G.L.; Wang, L. Review on the research progress of soil wind erosion erodibility. *China Soil Water Conserv. Sci.* **2022**, *20*, 143–150.
50. Chi, W.; Wang, Y.; Lou, Y.; Na, Y.; Luo, Q. Effect of Land Use/Cover Change on Soil Wind Erosion in the Yellow River Basin since the 1990s. *Sustainability* **2022**, *14*, 12930. [CrossRef]